Volatilome evolution during black truffle (*Tuber melanosporum*) ontogeny

Pedro MARCO [a,b], M. Ángeles SANZ [b,c], Eva TEJEDOR-CALVO[,d], Sergi GARCIA-BARREDA [a,b,*], Pierluigi CABONI [e], Santiago REYNA [f], Sergio SÁNCHEZ [a,b]

[a] Departamento de Ciencia Vegetal. Centro de Investigación y Tecnología Agroalimentaria de Aragón (CITA). Avda. Montañana 930, 50059 Zaragoza, Spain

[b] Instituto Agroalimentario de Aragón – IA2 (CITA-Universidad de Zaragoza), C/ Miguel Servet 177, 50013 Zaragoza, Spain

[c] Laboratories and Technological Assistance. Agrifood Research and Technology Centre of Aragon (CITA). Avda. Montañana 930, 50059 Zaragoza, Spain

[d] Laboratory for Flavor Analysis and Enology (LAAE), Department of Analytical Chemistry, Universidad de Zaragoza, C/ Pedro Cerbuna 12, 50009 Zaragoza, Spain

[e] Department of Life and Environmental Sciences. University of Cagliary. Via Ospedale 72, 09124 Cagliari, Italy

[f] ETS Ingeniería Agronómica y del Medio Natural. Universitat Politècnica de València. Camino de Vera s/n, 46021 Valencia, Spain

* Corresponding author. Tel.: (+34)976716371. E-mail: sgarciaba@cita-aragon.es

Abstract

The aroma is critical in the reproductive biology of truffles and in their commercial quality. However, previous research has almost exclusively focused on characterizing ripe ascocarps. We characterized the volatilome of the highly-prized black truffle (*Tuber melanosporum*) ascocarps from July, in an early development stage, to March, in the late harvesting season, and investigated the relationships among aroma, ascocarp growth and morphogenetic development. The aroma profile was analyzed using a head space gas chromatography technique coupled with mass spectrometer. Seventy-one volatile compounds were identified, with thirty of them being associated to specific development stages. Amongst those with higher occurrence, 4-penten-2-ol, dimethyl sulfide, ethyl acetate, 2-pentanol and 2-butanone were associated to ripe truffles, whereas methanethiol, isobutyl isobutyrate, butanedione and 3-methylanisole were associated to unripe truffles. Although each volatile showed specific temporal patterns, three development stages were clearly distinguished: unripe ascocarps of July-September, unripe ascocarps of October-December and ripe ascocarps of December-March.

Keywords: truffle, volatile organic compounds, ripening, aroma, morphogenesis, metabolomics, dimethyl sulfide

1. Introduction

The European black truffle (*Tuber melanosporum* Vittad.) is an ectomycorrhizal fungus that grows wild in northwestern Mediterranean countries, although nowadays practically all its production comes from cultivation (Garcia-Barreda, Camarero, et al., 2020; Reyna & Garcia-Barreda, 2014). These artificially-inoculated orchards have spread to many other countries, such as Australia or Argentina (Reyna & Garcia-Barreda, 2014; Tejedor-Calvo et al., 2023). It grows below ground, developing an intense aroma to attract animals that consume it and disperse its spores (Urban, 2016). The unique aroma of ripe black truffle is highly appreciated in high cuisine and has extensively been characterized. More than 100 volatile organic compounds (VOCs) have been identified, with the highest abundances being achieved by 2-methylbutanal, 3-methylbutanal, acetone, dimethyl sulfide (DMS) or methanethiol (Bellesia et al., 1998; Culleré et al., 2010; Talou et al., 1987; Tejedor-Calvo et al., 2021). This aroma can be affected by both pre-harvest and post-harvest practices (Campo et al., 2017; Hou et al., 2024; Tejedor-Calvo et al., 2023).

Truffle aroma is a critical component of truffle commercial quality and is key in the chemical ecology of truffles (Campo et al., 2017; Splivallo et al., 2011). Despite this, previous research has almost exclusively focused on characterizing the ripe stage (December-March), when ascocarps of commercial quality are harvested with the aid of trained dogs. Research on the evolution of the volatilome profile of truffles throughout ascocarp ontogeny is very scarce and mainly addresses species other than *T. melanosporum* (Caboni et al., 2020; Li et al., 2022; Zeppa et al., 2004). Studies on *T. melanosporum* ascocarp growth or evolution of biochemical parameters and gene expression are also scarce (Caboni et al., 2020; Harki et al., 2006; Montant et al., 1983; Pacioni et al., 1995; Zarivi et al., 2011, 2015).

The development of the truffle ascocarp has been explained with six morphogenetic stages, beginning with fruiting induction, mating and the very early stage of the ascocarp,

then followed by several stages during which the ascocarp develops and quickly swells, and completed with a stage in which the ascocarp matures and ripens (Garcia-Barreda, Camarero, et al., 2020; Le Tacon, 2017; Zarivi et al., 2015). Investigating the evolution of the volatilome profile throughout ascocarp ontogeny could help unraveling the complex relationships among ascocarp growth, maturity (linked to spore melanization) and ripeness (development of the typical aroma of ripe ascocarps), as well as the metabolic processes involved (Büntgen et al., 2021; Caboni et al., 2020; Martin et al., 2010). In this regard, the formation of the major *T. melanosporum* ascocarp odorants has been related to the truffle amino acid metabolism and fatty acid metabolism (Hou et al., 2024; Martin et al., 2010; Splivallo et al., 2011), although for some of them it has also been proposed some role of the microorganisms living in the truffle (Vahdatzadeh et al., 2015).

The main limitation for investigating truffle ascocarp ontogeny is its hypogeous habit, which makes it difficult to localize the samples, together with the destructive nature of these samplings and the high price of black truffle. In this regard, truffle nests provide unique opportunities for research, as already demonstrated (Murat et al., 2016; Taschen et al., 2022). Truffle nests is a cultivation practice consisting of amending the soil with peat in several points near the host tree (Garcia-Barreda, Marco, et al., 2020). These points frequently produce truffle ascocarps two or three years after establishing the nests (Murat et al., 2016; Taschen et al., 2022), thus making easier the ascocarp samplings and possible monitoring. Besides, in nests it is frequent to harvest clusters of ascocarps (ascocarps growing in close proximity, and thus being harvested together, when the trained dog localizes and marks one of them). These clusters are not exclusive of nests, but they are more frequent in them than in the bulk soil (Garcia-Barreda, Marco, et al., 2020). The occurrence of clusters in nests is subject to criticism from some growers, who think that clusters harbor ascocarps with contrasting levels of maturity and ripeness that are harvested and marketed together. Nests provide an

opportunity for the in-depth examination of the relationship among ascocarp development, maturation and ripeness.

In this study, we aim to characterize the evolution of the volatilome profile of *T. melanosporum* throughout the ascocarp ontogeny. For this, we took advantage of the ease to sample ascocarps in truffle nests. The VOC profile was determined for ascocarps harvested from July, in an early development stage, to March, in the late harvesting season, using a head space gas chromatography technique coupled with mass spectrometer (HS-GC-MS). We hypothesized that the VOC profile would be different in unripe and ripe ascocarps, and that ripeness markers could be identified. As a secondary aim, we characterized the temporal evolution of ascocarp weight and morphogenetic stages throughout this period. Finally, we examined ascocarp clusters to evaluate within-cluster differences in the VOC profile and the morphogenetic stages. We hypothesized that, during the harvesting season (December-March), clusters would harbor ascocarps with different VOC profiles.

2. Experimental procedures

2.1. Experimental site

The study was conducted in a truffle orchard in El Toro (Castellón province, eastern Spain, 1000 m a. s. l.), in the piedmont of Javalambre mountain range. The climate is Continental Mediterranean, with a mean annual temperature of 12.4 ºC and a mean annual rainfall of 510 mm. The soil is calcareous, with pH 7.9 and clay-loam texture, developed on a Quaternary colluvium consisting of locally derived clay, red sand and angular rock clasts (Table S1). The site lies within the natural distribution area of *T. melanosporum* (Garcia-Barreda et al., 2019).

A 1.5-ha plot of this orchard was used as an experimental plot in our study. The plot was planted in 2004 with holm oaks (*Quercus ilex* L. subsp. *ballota* Samp.) inoculated with *T. melanosporum*. The seedlings were planted at a density of 278 trees ha^{-1} (6 × 6 m planting

pattern). Since then, the soil has been shallowly tilled once a year in early spring. From the fifth year, the trees have been pruned every 3-4 years, and from the moment the plantation begun to produce truffles, at year six, the plantation has been irrigated with sprinkling during spring, summer and early autumn (April to October) each 3-4 weeks if there was no rainfall during those weeks. In the spring of 2015, the owner set up four truffle nests around each tree, at 1.2 m of distance from the host tree trunk. The installation of the nests consisted of digging holes about 30 cm deep, filling them with 1.5 L of a *Sphagnum* peat-based substrate (Especial Truficultura ® from Gramoflor: a 60% black peat – 40% white peat mix with pH raised to 7.5) and re-covering the substrate with soil. Ground ripe *T. melanosporum* ascocarps (1 g dry ascocarp per nest) were applied to the bulk soil – nest interphase before filling the hole with substrate. During the harvesting season November 2016 – March 2017 these nests produced their first truffles.

2.2. Experimental design and truffle sampling

The experimental plot was visited once a month from July 2017 to March 2018 and *T. melanosporum* ascocarps were harvested from the nests (sampling dates: 14 July, 7 August, 7 September, 9 October, 6 November, 17 December, 15 January, 20 February and 20 March). From July to November (before the harvesting season), we sampled unripe ascocarps. In December, (in the early harvesting season) we sampled both unripe and ripe ascocarps. From January to March (late harvesting season), we only sampled ripe ascocarps.

In each sampling, we randomly selected 12 trees. The sampling of unripe ascocarps (from July to December) consisted of carefully digging nests in the selected trees with a handheld shovel, after a dog trained to find truffles had looked over the nests without localizing any ripe or rotten ascocarp. The sampling of ripe ascocarps (from December to March) was done by an experienced truffle harvester with the aid of trained dogs. For the sake

of homogeneity of conditions between ripe and unripe ascocarps, only ascocarps growing in truffle nests were sampled.

In the field, the truffle ascocarps were kept refrigerated (4 ºC) immediately after being harvested. They were carried to the laboratory and cleaned by gently brushing under fresh tap water and by 15 min of ultrasound treatment. Then the ascocarps were surface air dried and cooled at 7 ºC on separate containers until further analyses. Only healthy ascocarps without abiotic or biotic damages (resulting in rotting, softened texture or galleries) were selected for the study, thus resulting in a total of 83 truffle ascocarps: 47 unripe and 36 ripe ones (Table S2).

For each ascocarp, the following data were collected: date of sampling, whether the dig was marked by the dog (the aroma was developed at least in one ascocarp) or not, and the ascocarp weight. When digging a nest, sometimes only one ascocarp was found (single dig), whereas in other cases several truffles growing in close proximity (ascocarp clusters) were found. This was also annotated (Table S2) and ascocarps in clusters were used to assess the variability in VOC profiles and morphogenetic stage within an ascocarp cluster. Sixteen clusters (eight unripe and eight ripe), including 47 ascocarps (25 unripe and 22 ripe), were used for this aim (Table S2). Finally, the morphogenetic stage of the ascocarp was assessed from a gleba sample, following the criteria of Zarivi et al. (2015) and Le Tacon (2017) (Table 1).

2.3. HS-GC-MS analysis

A total of 83 ascocarps were used for the HS-GC-MS analysis. Each sampling included a minimum of three ascocarps except for July, when only one of the ascocarps found weighted more than 10 g (Table S2). Ascocarps smaller than 10 g were excluded because they would be problematic for the subsequent methodologies (that included six ascocarps found in July that

weighted 0.08 to 3.0 g, and six in August that weighted 0.3 to 4.7 g). Only healthy ascocarps were used, and in all cases the HS-GC-MS analysis was carried out during the 48 hours following the field sampling.

The VOC profile was analyzed by static headspace technique using a Turbomatrix HS16 sampler (PerkinElmer, Massachusetts, USA). Briefly, for each ascocarp 4 g of gleba sample was placed in a 20 ml vial and hermetically closed. Headspace was programmed to 120 ºC for 15 min and 1 min of pressurization time. The injection was carried out over 6 s at 20 psi and an inlet temperature of 220 °C. The headspace sampler was connected to a Clarus 500 Gas Chromatography system coupled with a Mass Spectrometer (PerkinElmer, Massachusetts, USA) equipped with a DB-Wax capillary column (60 m × 0.25 mm i.d. × 0.25 µm film thickness) (Agilent Technologies, California, USA). A flow of 1 mL/min was used with helium as a carrier gas. The oven temperature was 45 °C for 2 min, raised to 110 °C at a rate of 7 °C/min, and finally to 225 °C at 25 °C/min, and held for 5 min. The mass spectrometer used the electron impact mode with an ionization potential of 70 eV and an ion source temperature of 200 °C. The interface temperature was 220 °C. The mass spectrometer scanning was recorded in full scan mode (35–300 m/z). A TurboMass ver. 5.4.2 software was used for controlling the gas chromatography – mass spectrometer system. Peak identification of the volatile components was achieved by comparison of the mass spectra with mass spectral data from the NIST MS Search Program 2.0 library and by comparison of previously reported Retention Index (RI) with those calculated using an n-alkane (C6-C20) series under the same analysis conditions. Semiquantification of the VOCs was done by integrating the area of one ion characteristic of each compound and normalization by calculating the relative percentage.

2.4. Statistical analysis

To analyze the evolution of the VOC profile throughout the ascocarp development, partial least-squares discriminant analysis (PLS-DA) was performed using R and the ropls package(R Core Team, 2023; Thévenot et al., 2015). For the PLS-DA analysis, the truffle ascocarps were grouped according to their development stage into: (a) unripe ascocarps sampled from July to September (early development/swelling stage), (b) unripe ascocarps sampled from October to December (late development/swelling stage), and (c) ripe ascocarps sampled from December to March (maturation stage). This grouping yielded higher predictive performance and goodness of fit than grouping ascocarps in ripe/unripe ascocarps or in morphogenetic stages.

The existence of outliers in the PLS-DA model was explored with an observation diagnostic plot, which shows the distances within and orthogonal to the projection plane, but no outlier was identified. The predictive performance of the model was assessed with the cumulative Q2Y parameter and its goodness of fit with the cumulative R2Y parameter. The final number of components of the PLS-DA model was determined by the increase in Q2Y and R2Y when a new component was added to the model (Thévenot et al., 2015). To avoid overfitting, a permutation testing to estimate the significance of Q2Y and R2Y was used. To complement the evaluation of the predictive performance of the model, we trained the model on a randomly selected subset of 6/7 of the samples (n = 71). Then, we computed the performance of this model on the training subset and on the validation subset (the remaining 1/7 of the samples, n = 12). The contribution of the different VOCs to the separation of the three groups was determined with the VIP metric (variable importance in projection). The VIP_{pred}, which measures the variable importance in prediction, was used in this case (Galindo-Prieto et al., 2014). A VIP score higher than one was considered the threshold to determine discriminant variables in the model (Kieffer et al., 2016).

For the VOCs with $VIP_{pred} > 1$, an additive model (AM) with a Gaussian (normal) error distribution was used to analyze the evolution of the relative percentage area throughout the ascocarp development. Time was treated as a smoothed predictor, specified using a shrinkage smoother (cubic regression spline). The assumptions of normal distribution and constant variance were tested, and the response variable was square-root or log-transformed when necessary. In a few extreme cases, these transformations were not suitable and a generalized additive model (GAM) with a Gamma error distribution was used. The AM and GAM analyses were conducted with the package mgcv in R (Wood, 2011). An AM was also used to analyze the evolution of ascocarp weight throughout ascocarp ontogeny.

Finally, in order to explore the hypothesis that ascocarp clusters include ascocarps at different points of ripeness, a principal component analysis (PCA) was used to compare the VOC profile of the ascocarps sampled in each of the monthly samplings. The PCAs were plotted with the package factoextra in R (Kassambara & Mundt, 2020).

3. Results

The weight of the ascocarps increased significantly from July to October, according to the AM ($F = 8.8$, $P < 0.001$, $n = 114$, Fig. 1a). From that moment, the weight did not significantly change, although some fluctuations among samplings were found (Fig. 1a, Fig. S1). The analysis of the morphogenetic stage (Fig. 2, Fig. S2) showed that different stages could be present in the soil at the same time, mainly during late summer: stage 4 was found from July to September, stage 5 from August to October, substage 6a from September to December, and substage 6b-c from December to March (Fig. 1b). It is also noteworthy that stage 3 was found in July and August, although these ascocarps were not included in the VOC analysis due to their small size (0.08 to 1.8 g). As a side note, during the sampling of unripe ascocarps

(sampling of nests in which the dogs had not localized ripe ascocarps) from July to December, we found *T. melanosporum* ascocarps in 29-45% of the sampled nests (Table S3).

A total of 71 VOCs were identified by HS-GC-MS in the 83 truffle ascocarps studied (Table 2). The selected PLS-DA model analyzing the evolution of VOC profile throughout the ascocarp development was based on four components (Fig. S3a). The first PLS-DA component clearly separated the July to September unripe ascocarps from the ripe ascocarps, with the October to December unripe ascocarps in an intermediate position. The second component separated the October to December unripe ascocarps from the other unripe and ripe ascocarps (Fig. 2a). Thirty of the VOCs presented VIP_{pred} scores higher than one (Fig. 2b). Fourteen of them were negatively associated with the first PLS-DA component, 11 were positively associated with the first component, four were negatively associated with the second component and one was positively associated with the second component (Fig. 3). The cumulative R2Y of the model was 0.834 and the cumulative Q2Y was 0.731, both being significantly higher ($P < 0.01$) than the values obtained by the random permutation test (Fig S3b). According to the validation test, 96% of the calibration subsample and 83% of the validation subsample were properly classified in their respective groups.

The most abundant VOCs in unripe ascocarps from July to September were methanethiol (19.2%), 4-penten-2-ol (11.3%), acetone (10.6%), ethanol (9.3%), isobutyraldehyde (6.1%) and isobutyl isobutyrate (5.8%) (Fig. 4). Among these, only methanethiol and isobutyl isobutyrate showed a positive association with this period, according to the VIP_{pred} (Fig. 2b). The AMs indicated that both had a peak between September and October, with much lower contribution to the VOC profile in other periods (Fig. 5a, c). Many other VOCs with lower relative abundance were associated with this period, among them butanedione (3.9%), which steadily decreased through time; 3-methylanisole (2.6%),

which had a peak in August-September; and furfural (2.5%), which was abundant in July-September (Fig. 5, Fig. S4).

The most abundant VOCs in unripe ascocarps from October to December were 4-penten-2-ol (21.3%), methanethiol (20.3%), ethanol (12.7%), acetone (6.3%) and ethyl acetate (5.9%) (Fig. 4). None of them associated with this period according to the VIP_{pred} (Fig. 2b). However, a few VOCs with lower abundance were associated with this period, such as 2-heptanone (1.0%), with a peak in October-November; and 2-methyl-1-butanol, with an October peak (Fig. S5b, c). On the other hand, dimethyl disulfide (DMDS) was negatively associated with this period according to the VIP_{pred}, presenting 0.10% relative abundance in unripe ascocarps of October-December and 0.30% in the other two analyzed periods (Fig. S5e).

The most abundant VOCs in ripe ascocarps were 4-penten-2-ol (16.9%), dimethyl sulfide (16.2%), ethanol (9.5%), ethyl acetate (8.5%), 2-pentanol (8.2%), 2-butanone (5.9%), methanethiol (5.9%) and 2-methylbutanal (5.3%) (Fig. 4). Among these, 4-penten-2-ol, DMS, ethyl acetate, 2-pentanol and 2-butanone showed a positive association with ripe truffles according to the VIP_{pred} (Fig. 2b). The AMs indicated that 4-penten-2-ol, ethyl acetate and 2-butanone gradually increased through time, whereas DMS presented a December-January peak and 2-pentanol presented a February peak (Fig. 6). Several other VOCs with lower relative abundance were associated with ripe truffles, among them butanal (1.8%), 1-propanol (0.9%) or 2-pentanone (0.8%) (Fig. 6b, Fig. S6a, b).

Finally, a PCA was performed for the VOC profile of each one of the sampling months in which ascocarps clusters were found. August data is not shown because the low number of samples did not allow for clear comparisons among ascocarps. From September to January (although not in February), the first PCA component (PC1) was positively associated with VOCs such as 4-penten-2-ol, ethyl acetate, 2-pentanone or ethyl 2-methylbutanoate (which in

the PLS-DA analysis were linked to ripe truffles) and negatively associated with VOCs such as butanedione, isobutyl isobutyrate, 3-methylanisole, furfural or 2-octen-4-one (which in PLS-DA were linked to unripe truffles) (Fig. 7).

In September, two ascocarp clusters were found. One of them comprised two ascocarps, both with a similar position in the PCA biplot with respect to PC1 (ascocarps S4a, S4b, Fig. 7a) despite presenting different morphogenetic stage (stage 5 for ascocarp S4a and substage 6a for S4b). The other one comprised seven ascocarps, all of them with a similar position with respect to PC1 except for one (S7a, Fig. 7a). Three of these ascocarps were in morphogenetic stage 4 (S7c, S7d and S7g), one in stage 5 (S7f) and three in substage 6a (S7a, S7b and S7e). In October, only one cluster was found, with two ascocarps showing a similar position with respect to PC1 despite presenting different morphogenetic stage (stage 5 for O3a and substage 6a for O3b) (Fig. 7b). In November, two clusters were found, both of them with ascocarps showing contrasting positions with respect to PC1 (Fig. 7c) despite all being in the same morphogenetic stage (6a). In December, one of the clusters (marked by the trained dogs) comprised ascocarps with contrasting positions with respect to PC1 and different morphogenetic substage (6a for D7b, 6b-c for D7a and D7c, Fig. 7d). Another cluster (not marked by dogs) comprised ascocarps with contrasting positions with respect to PC1 despite all being in the same morphogenetic stage (6b-c for D13a to D13d, Fig. 7d). The other four clusters sampled in December (three marked by dogs and one not marked) comprised ascocarps with a similar position with respect to PC1 (Fig. 7d) and in the same morphogenetic stage (6b-c). The four clusters sampled in January and February comprised ascocarps with similar positions with respect to PC1 (Fig. 7e, f) and in the same morphogenetic stage (6b-c).

4. Discussion

This study is the first to characterize the evolution of the volatilome profile of *T. melanosporum* throughout the ascocarp ontogeny from July to March. This allowed the

identification of several ripeness markers, both amongst the dominant VOCs such as 4-penten-2-ol, DMS, ethyl acetate, 2-pentanol or 2-butanone and amongst the lower-abundance VOCs such as butanal. The role of many of these VOCs in the aroma of ripe *T. melanosporum* was already highlighted by previous research (Culleré et al., 2010; Talou et al., 1987). We also characterized the VOC profile of *T. melanosporum* ascocarps during early development stages, identifying VOCs such as methanethiol, isobutyl isobutyrate, butanedione or 3-methylanisole as markers of these stages. This information is relevant for studies of the chemical ecology of truffles and studies of metabolic processes during truffle development (Martin et al., 2010; Splivallo et al., 2011; Zeppa et al., 2004).

In our study, some of these VOCs showed a progressive increase or decrease throughout ascocarp ontogeny (e. g. butanal, 2-butanone, 4-penten-2-ol, ethyl acetate or butanedione), whereas other ones showed high relative abundance during limited periods (e. g. 3-methylanisole, furfural and 4-sec-butylphenol in August-September; methanethiol and isobutyl isobutyrate in September-October; DMS in early harvesting season or 2-pentanol in late harvesting season).

The 71 VOCs identified in the study included the major odorants of black truffle, such as DMS, DMDS, 2-methylbutanal, 3-methylbutanal, butanedione, ethyl 2-methylbutanoate or ethyl isovalerate (Culleré et al., 2010, 2013; Tejedor-Calvo et al., 2021). Among the 30 VOCs that showed significant time trends throughout the truffle ascocarp ontogeny, six were alcohols, six ketones and four aldehydes. In general, the VOCs characterizing early development stages consisted of longer carbon chains (e. g. 1-octanol, 2-octen-4-one, nonanal) than those characterizing the ripe stage (e. g. 2-pentanol, 2-butanone, butanal), with the notable exception of butanedione. Besides, aromatic compounds and heterocyclic compounds were more frequently linked to early development stages (e. g. 2-pentylfuran, 3-methylanisole, furfural).

Regarding sulfur compounds, our study showed clear time patterns for methanethiol and DMS. These VOCs, as well as DMDS, are considered products of the methionine catabolism (Liu et al., 2013; Martin et al., 2010). The relative abundance of methanethiol reaches its peak during intermediate development stages, whereas DMS reaches its peak later, during early maturation. This agrees with their hypothesized roles in methionine catabolism (Martin et al., 2010). L-methionine is transformed into 3-(metylthio)-propanal after transamination and decarboxylation, and then due to a reduction step into methanethiol, DMS and DMDS (Splivallo et al., 2011). The DMS peak matches with methionine and cysteine peaks in black truffle (Caboni et al., 2020; Harki et al., 2006). Dimethyl sulfide is a powerful attractant for animals consuming truffle ascocarps (Pacioni et al., 1991; Splivallo et al., 2011). The temporal pattern we found could explain why damages by truffle beetle or wild boar are more frequent in early harvesting season or even in the immediately preceding months (Garcia-Barreda, Marco, et al., 2020; Piattoni et al., 2016).

Important odorants of truffles such as 2-methylbutanal, 2-methyl-1-butanol, 3-methylbutanal or butanedione have been linked to the catabolism of amino acids such as leucine or isoleucine via the Ehrlich pathway (Caboni et al., 2020; Martin et al., 2010; Vahdatzadeh & Splivallo, 2018). As an example, isoleucine, after transamination and decarboxylation steps is transformed into 2-methylbutanal, and then to 2-methyl-1-butanol due to a reduction step. In our study, only 2-methyl-1-butanol, with a peak in October, and butanedione, with a progressive decrease from August to March, showed clear time trends, suggesting that the corresponding metabolic reactions are happening in intermediate stages of the ascocarp ontogeny. These trends contrast with those of leucine and isoleucine, which are more abundant in late maturation stages (Harki et al., 2006). The 2-methylbutanal, 2-methyl-1-butanol and 3-methylbutanal show phytotoxic effects on herbaceous species, which may

play a role in alleviating the competition of roots on truffle during ascocarp development (Pacioni et al., 1995).

Zeppa et al. (2004) linked the occurrence in truffles of methyl ketones and C8-compounds such as 1-octen-3-ol to the metabolism of fatty acids such as the linoleic acid. In our study, 2-butanone and 2-pentanone reached their peaks in ripe ascocarps, coinciding with the maximum levels of linoleic acid in black truffle (Caboni et al., 2020). By contrast, C8-compounds were more frequently linked to early development stages, unlike what happens in other close *Tuber* species (Lu et al., 2021). Besides, the β-oxidation of long-chain saturated fatty acids has been proposed as a source of acetic and butanoic acids, their corresponding alcohols and acetate esters in fungi (Hou et al., 2024).

Our study clearly separated the VOC profile of three different groups: unripe ascocarps of July-September, unripe ascocarps of October-December and ripe ascocarps (December-March). During the July-September period, ascocarps quickly increased their weight, in agreement with previous observations in France (Montant et al., 1983). Besides, in our study the July-September period was characterized by the coexistence of several morphogenetic stages (in our case, stages 3, 4, 5 and 6a), which agrees with that previously found in Italy (Zarivi et al., 2015). The latter could be related to the hypothesis that the induction of most ascocarps occurs in several flushes during May-June (Pacioni et al., 2014). It is also noteworthy that the ascocarp weight in August was much higher in our study than in Montant et al. (1983), in line with the fact that we found ascocarps in morphogenetic stages 4, 5 and 6a one month earlier than Zarivi et al. (2015). This suggests an earlier or more rapid development and swelling of ascocarps in our study, which could be related to higher temperatures in Spain or to the use of truffle nests (Garcia-Barreda et al., 2012; Garcia-Barreda, Marco, et al., 2020).

Regarding the October-December period, our results suggest that truffles finished swelling during October. From that moment the mean weight of the sampled ascocarps underwent a series of fluctuations, which could be related to the high variability of truffle size in plantations (Garcia-Barreda et al., 2021; Garcia-Barreda, Marco, et al., 2020). According to Montant et al. (1983) and Zarivi et al. (2015), *T. melanosporum* ascocarp would reach its final size during morphogenetic stage 5 (September-early November), then entering the maturation and ripening stage. Our data agree with this view: in the September sampling, 62% of the ascocarps were in stages 4-5 and the weight increase was quick; in October 27% of the ascocarps were in stage 5 and the weight increase begun to slow down; whereas in November all ascocarps were already in substage 6a and no weight increase was observed. Previous research already pointed out the absence of causal links between ascocarp weight and spore maturity (Garcia-Barreda et al., 2021), as well as the key regulatory role of tyrosinase in maturation (Miranda et al., 1997).

In December, almost all ascocarps reached morphogenetic substage 6b-c. Previous research already showed that spore maturity quickly increases during November and early December (Garcia-Barreda, Marco, et al., 2020). In that study, the confidence band for the temporal trend of spore maturity was relatively narrow, suggesting a high degree of synchronization in the maturation process. This agrees with our observation of a simultaneous passage of almost all ascocarps from substage 6a in November to substage 6b-c in December. Despite this, not all ascocarps were marked by the dogs during December, many of them achieved ripeness and were harvested in January-March. This suggests that spore maturation and ripe aroma development, although chronologically overlapping, are not completely in sync.

We analyzed eight ascocarp clusters localized from December to February by trained dogs (this indicating that at least one of the ascocarps was ripe). For all the January and

411 February clusters (with 2-3 ascocarps each), every ascocarp presented morphogenetic
412 substage 6b-c, and all clusters comprised ascocarps with similar VOC profiles. The same
413 happened for three of the four clusters harvested in December (with 2-4 ascocarps each). The
414 only exception was a cluster in which one of the ascocarps was in substage 6a and showed a
415 VOC profile very different from the other two ascocarps (in substage 6b-c). This suggests that
416 in a cluster harvested with trained dogs in December-February (the harvesting season), all
417 ascocarps share a similar degree of ripeness if they present high spore maturity, at least for
418 clusters of 2-4 ascocarps.

419 The situation was very different in clusters of unripe ascocarps. The two clusters
420 sampled in December that were not localized by trained dogs, were formed by ascocarps in
421 morphogenetic substage 6b-c, but one of them presented distinct VOC profiles (one ascocarp
422 grouping with those linked to VOCs of ripe truffles and the remaining with unripe truffles). A
423 similar situation was found in November, although with all ascocarps in substage 6a. In
424 September-October, clusters included different morphogenetic stages and distinct VOC
425 profiles. This suggests that within a cluster there are ascocarps generated in different flushes
426 (Pacioni et al., 2014) or that develop at different paces.

427 Our study took advantage of the ease of finding ascocarps in truffle nests. In our study,
428 29-45% of the nests sampled in July-November (without dog mark, and thus randomly
429 selected) presented ascocarps, three years after the nests were set up. This percentage explains
430 the good reputation of nests among growers, although they are not free from criticism. One of
431 them is the lower maturity and ripeness that some growers attribute to cluster ascocarps. In
432 our study, we found no variability of spore maturity or VOC profile within clusters of
433 January-February. The problem seems concentrated in early season, at least for clusters with
434 up to four ascocarps. This is no trivial matter, since nest ascocarps are more frequently
435 harvested in early season (Garcia-Barreda, Marco, et al., 2020).

To conclude, we characterized the evolution of the volatilome profile of *T. melanosporum* throughout the ascocarp ontogeny, identifying 30 VOCs as markers of the development stage of the truffle. Amongst the dominant VOCs, 4-penten-2-ol, DMS, ethyl acetate, 2-pentanol and 2-butanone were associated to ripe truffles, whereas methanethiol, isobutyl isobutyrate, butanedione and 3-methylanisole were associated to unripe truffles. The temporal evolution of these VOCs throughout the ascocarp ontogeny was modeled, with each VOC showing specific patterns, although three development stages were clearly distinguished: unripe ascocarps of July-September, unripe ascocarps of October-December and ripe ascocarps. During July-September, the ascocarps rapidly increased their weight, and several morphogenetic stages coexisted. During October-December the ascocarps finished their weight increase and then begun to mature, with the aroma typical of ripe ascocarps being achieved in December-March. Finally, we found that in clusters of 2-4 ascocarps that were marked by trained dogs during the harvesting season, ascocarps presented the same maturation degree and VOC profile, except for one cluster in early season.

CRediT authorship contribution statement

Pedro Marco: Conceptualization, Methodology, Investigation, Writing – original draft. **María Ángeles Sanz**: Investigation, Formal analysis, Writing – review & editing. **Eva Tejedor-Calvo:** Formal analysis, Writing – original draft. **Sergi Garcia-Barreda:** Conceptualization, Methodology, Investigation, Formal analysis, Writing – original draft. **Pierluigi Caboni:** Formal analysis, Writing – review & editing. **Santiago Reyna:** Investigation, Writing – review & editing. **Sergio Sánchez:** Conceptualization, Methodology, Investigation, Writing – original draft, Funding acquisition.

Declaration of competing interest

The authors declare that they have no known competing financial interests or personal relationships that could have appeared to influence the work reported in this paper.

Data availability

Datasets generated during the current study are available from the corresponding author on reasonable request.

Funding

This work was supported by the Spanish Institute for Agronomical Research (INIA) [grant number RTA2015-0053-00-00] and the Spanish Ministry of Science and Innovation (MCIN) [grant number PID2022-139407OR-I00]. The participation of E. T.-C. was supported by a Juan de la Cierva grant of MCIN [grant number JDC2022-048252-I].

References

Acree, T., & Arn, H. (2004). *Flavornet and Human Odor Space*. http://www.flavornet.org/flavornet

Bellesia, F., Pinetti, A., Bianchi, A., & Tirillini, B. (1998). The volatile organic compounds of black truffle (*Tuber melanosporum* Vitt.) from middle Italy. *Flavour and Frangance Journal*, *13*(1), 56–58.

Büntgen, U., Peter, M., Tegel, W., Stobbe, U., Elburg, R., Sproll, L., Molinier, V., Čejka, T., Isaac, E. L., & Egli, S. (2021). Eco-archaeological excavation techniques reveal snapshots of subterranean truffle growth. *Fungal Biology*, *125*(12), 951–961. https://doi.org/10.1016/J.FUNBIO.2021.09.001

Caboni, P., Scano, P., Sanchez, S., Garcia-Barreda, S., Corrias, F., & Marco, P. (2020). Multi-platform metabolomic approach to discriminate ripening markers of black truffles (*Tuber melanosporum*). *Food Chemistry*, *319*, 126573. https://doi.org/10.1016/j.foodchem.2020.126573

Campo, E., Marco, P., Oria, R., Blanco, D., & Venturini, M. E. (2017). What is the best method for preserving the genuine black truffle (*Tuber melanosporum*) aroma? An olfactometric and sensory approach. *LWT - Food Science and Technology*, *80*, 84–91. https://doi.org/10.1016/j.lwt.2017.02.009

Culleré, L., Ferreira, V., Chevret, B., Venturini, M. E., Sánchez-Gimeno, A. C., & Blanco, D. (2010). Characterisation of aroma active compounds in black truffles (*Tuber*

melanosporum) and summer truffles (*Tuber aestivum*) by gas chromatography–olfactometry. *Food Chemistry*, *122*(1), 300–306. https://doi.org/10.1016/J.FOODCHEM.2010.02.024

Culleré, L., Ferreira, V., Venturini, M. E., Marco, P., & Blanco, D. (2013). Potential aromatic compounds as markers to differentiate between *Tuber melanosporum* and *Tuber indicum* truffles. *Food Chemistry*, *141*(1), 105–110. https://doi.org/10.1016/J.FOODCHEM.2013.03.027

Galindo-Prieto, B., Eriksson, L., & Trygg, J. (2014). Variable influence on projection (VIP) for orthogonal projections to latent structures (OPLS). *Journal of Chemometrics*, *28*(8), 623–632. https://doi.org/10.1002/CEM.2627

Garcia-Barreda, S., Camarero, J. J., Vicente-Serrano, S. M., & Serrano-Notivoli, R. (2020). Variability and trends of black truffle production in Spain (1970-2017): linkages to climate, host growth, and human factors. *Agricultural and Forest Meteorology*, *287*, 107951. https://doi.org/10.1016/j.agrformet.2020.107951

Garcia-Barreda, S., Marco, P., Martín-Santafé, M., Tejedor-Calvo, E., & Sánchez, S. (2020). Edaphic and temporal patterns of *Tuber melanosporum* fruitbody traits and effect of localised peat-based amendment. *Scientific Reports*, *10*(1), 4422. https://doi.org/10.1038/s41598-020-61274-x

Garcia-Barreda, S., Reyna, S., Pérez-Badía, R., Rodríguez-Barreal, J. A., & Domínguez-Núñez, J. A. (2012). Ecología de la trufa y las áreas truferas. In S. Reyna (Ed.), *Truficultura: Fundamentos y técnicas* (2nd ed., pp. 151–206). Ed. Mundi-Prensa.

Garcia-Barreda, S., Sánchez, S., Marco, P., Benucci, G. M. N., & González, V. (2021). Lack of linkages among fruiting depth, weight, and maturity in irrigated truffle fungi marks the complexity of relationships among morphogenetic stages. *Journal of Fungi*, *7*(2), 102. https://doi.org/10.3390/jof7020102

Garcia-Barreda, S., Sánchez, S., Marco, P., & Serrano-Notivoli, R. (2019). Agro-climatic zoning of Spanish forests naturally producing black truffle. *Agricultural and Forest Meteorology*, *269–270*, 231–238. https://doi.org/10.1016/j.agrformet.2019.02.020

Harki, E., Bouya, D., & Dargent, R. (2006). Maturation-associated alterations of the biochemical characteristics of the black truffle *Tuber melanosporum* Vitt. *Food Chemistry*, *99*(2), 394–400. https://doi.org/10.1016/J.FOODCHEM.2005.08.030

Hou, Z., Xia, R., Li, Y., Xu, H., Wang, Y., Feng, Y., Pan, S., Wang, Z., Ren, H., Qian, G., Wang, H., Zhu, J., & Xin, G. (2024). Key components, formation pathways, affecting factors, and emerging analytical strategies for edible mushrooms aroma: A review. *Food Chemistry*, *438*, 137993. https://doi.org/10.1016/J.FOODCHEM.2023.137993

Kassambara, A., & Mundt, F. (2020). *Factoextra: extract and visualize the results of multivariate data analyses*. https://CRAN.R-project.org/package=factoextra

Kieffer, D. A., Piccolo, B. D., Vaziri, N. D., Liu, S., Lau, W. L., Khazaeli, M., Nazertehrani, S., Moore, M. E., Marco, M. L., Martin, R. J., & Adams, S. H. (2016). Resistant starch alters gut microbiome and metabolomic profiles concurrent with amelioration of chronic

kidney disease in rats. *American Journal of Physiology - Renal Physiology*, *310*(9), F857–F871. https://doi.org/https://doi.org/10.1152/ajprenal.00513.2015

Le Tacon, F. (2017). *Les truffes: Biologie, écologie et domestication*. AgroParisTech.

Li, Y., Li, J., Qiao, P., Zhou, D., Xing, Y., & Chen, J. (2022). Monitoring the volatile composition and change in different geographical regions and harvest time of Chinese truffle (*Tuber indicum* Cooke & Massee). *European Food Research and Technology*, *248*(6), 1663–1677. https://doi.org/10.1007/S00217-022-03994-0

Liu, R. S., Zhou, H., Li, H. M., Yuan, Z. P., Chen, T., & Tang, Y. J. (2013). Metabolism of l-methionine linked to the biosynthesis of volatile organic sulfur-containing compounds during the submerged fermentation of Tuber melanosporum. *Applied Microbiology and Biotechnology*, *97*(23), 9981–9992. https://doi.org/10.1007/S00253-013-5224-Z

Lu, B., Perez-Moreno, J., Zhang, F., Rinaldi, A. C., & Yu, F. (2021). Aroma profile of two commercial truffle species from Yunnan and Sichuan, China: inter- and intraspecific variability and shared key compounds. *Food Science and Human Wellness*, *10*(2), 163–173. https://doi.org/10.1016/J.FSHW.2021.02.005

Martin, F., Kohler, A., Murat, C., Balestrini, R., Coutinho, P. M., Jaillon, O., Montanini, B., Morin, E., Noel, B., Percudani, R., Porcel, B., Rubini, A., Amicucci, A., Amselem, J., Anthouard, V., Arcioni, S., Artiguenave, F., Aury, J. M., Ballario, P., … Wincker, P. (2010). Périgord black truffle genome uncovers evolutionary origins and mechanisms of symbiosis. *Nature*, *464*(7291), 1033–1038. https://doi.org/10.1038/nature08867

Miranda, M., Zarivi, O., Bonfigli, A., Amicarelli, F., Aimola, P., Ragnelli, A. M., & Pacioni, G. (1997). Melanogenesis, tyrosinase expression, and reproductive differentiation in black and white truffles (Ascomycotina). *Pigment Cell Research*, *10*(1–2), 46–53. https://doi.org/10.1111/j.1600-0749.1997.tb00465.x

Montant, C., Kulifaj, M., & Gleize, R. (1983). Note sur la recolte de jeunes ascocarpes du *Tuber melanosporum* Vitt. (truffe noire de Périgord) et leur evolution. *Comptes Rendus de l'Académie Des Sciences. Série III, Sciences de La Vie*, *296*, 463–468.

Murat, C., Bonneau, L., Varga, H. D. La, Olivier, J.-M., Sandrine, F., & Le Tacon, F. (2016). Trapping truffle production in holes: a promising technique for improving production and unravelling truffle life cycle. *Italian Journal of Mycology*, *45*(1), 47–53. https://doi.org/10.6092/issn.2531-7342/6346

Pacioni, G., Bologna, M. A., & Laurenzi, M. (1991). Insect attraction by *Tuber*: a chemical explanation. *Mycological Research*, *95*(12), 1359–1363. https://doi.org/10.1016/S0953-7562(09)80385-7

Pacioni, G., Leonardi, M., Di Carlo, P., Ranalli, D., Zinni, A., & De Laurentiis, G. (2014). Instrumental monitoring of the birth and development of truffles in a *Tuber melanosporum* orchard. *Mycorrhiza*, *24*(S1), 65–72. https://doi.org/10.1007/s00572-014-0561-z

Pacioni, G., Ragnelli, A. M., & Miranda, M. (1995). Truffle development and interactions with the biotic environment. In V. Stocchi, P. Bonfante, & M. Nuti (Eds.), *Biotechnology*

574 *of Ectomycorrhizae* (pp. 213–227). Plenum Press. https://doi.org/10.1007/978-1-4615-
575 1889-1_19

576 Piattoni, F., Ori, F., Amicucci, A., Salerni, E., & Zambonelli, A. (2016). Interrelationships
577 between wild boars (*Sus scrofa*) and truffles. In A. Zambonelli, M. Iotti, & C. Murat
578 (Eds.), *True Truffle (*Tuber spp.*) in the World*. Springer, Cham.

579 R Core Team. (2023). *R: a language and environment for statistical computing*. R
580 Foundation for Statistical Computing. https://www.r-project.org/

581 Reyna, S., & Garcia-Barreda, S. (2014). Black truffle cultivation: a global reality. *Forest*
582 *Systems*, *23*(2), 317–328. https://doi.org/10.5424/fs/2014232-04771

583 Splivallo, R., Ottonello, S., Mello, A., & Karlovsky, P. (2011). Truffle volatiles: from
584 chemical ecology to aroma biosynthesis. *New Phytologist*, *189*(3), 688–699.
585 https://doi.org/10.1111/j.1469-8137.2010.03523.x

586 Talou, T., Delmas, M., & Gaset, A. (1987). Principal constituents of black truffle (*Tuber*
587 *melanosporum*) aroma. *Journal of Agricultural and Food Chemistry*, *35*, 774–777.
588 https://doi.org/https://doi.org/10.1021/jf00077a031

589 Taschen, E., Callot, G., Savary, P., Sauve, M., Penuelas-Samaniego, Y., Rousset, F., Parladé,
590 X., Selosse, M. A., & Richard, F. (2022). Efficiency of the traditional practice of traps to
591 stimulate black truffle production, and its ecological mechanisms. *Scientific Reports*, *12*,
592 16201. https://doi.org/10.1038/s41598-022-19962-3

593 Tejedor-Calvo, E., García-Barreda, S., Sánchez, S., Morales, D., Soler-Rivas, C., Ruiz-
594 Rodriguez, A., Sanz, M. Á., Garcia, A. P., Morte, A., & Marco, P. (2021). Supercritical
595 CO_2 extraction method of aromatic compounds from truffles. *LWT*, *150*, 111954.
596 https://doi.org/10.1016/J.LWT.2021.111954

597 Tejedor-Calvo, E., Garcia-Barreda, S., Sebastián Dambolena, J., Pelissero, D., Sánchez, S.,
598 Marco, P., & Nouhra, E. (2023). Aromatic profile of black truffle grown in Argentina:
599 Characterization of commercial categories and alterations associated to maturation,
600 harvesting date and orchard management practices. *Food Research International*, *173*,
601 113300. https://doi.org/10.1016/J.FOODRES.2023.113300

602 Thévenot, E. A., Roux, A., Xu, Y., Ezan, E., & Junot, C. (2015). Analysis of the human adult
603 urinary metabolome variations with age, body mass index, and gender by implementing
604 a comprehensive workflow for univariate and OPLS statistical analyses. *Journal of*
605 *Proteome Research*, *14*(8), 3322–3335.
606 https://doi.org/10.1021/ACS.JPROTEOME.5B00354

607 Urban, A. (2016). Truffles and Small Mammals. In A. Zambonelli, M. Iotti, & C. Murat
608 (Eds.), *True Truffle (Tuber spp.) in the World* (pp. 353–373). Springer, Cham.
609 https://doi.org/10.1007/978-3-319-31436-5_21

610 Vahdatzadeh, M., Deveau, A., & Splivallo, R. (2015). The role of the microbiome of truffles
611 in aroma formation: A meta-analysis approach. *Applied and Environmental*
612 *Microbiology*, *81*(20), 6946–6952. https://doi.org/10.1128/AEM.01098-15

613 Vahdatzadeh, M., & Splivallo, R. (2018). Improving truffle mycelium flavour through strain
614 selection targeting volatiles of the Ehrlich pathway. *Scientific Reports*, *8*(1), 9304.
615 https://doi.org/10.1038/s41598-018-27620-w

616 Wood, S. N. (2011). Fast stable restricted maximum likelihood and marginal likelihood
617 estimation of semiparametric generalized linear models. *Journal of the Royal Statistical*
618 *Society (B)*, *73*(1), 3–36. https://doi.org/https://doi.org/10.1111/j.1467-
619 9868.2010.00749.x

620 Zarivi, O., Bonfigli, A., Colafarina, S., Aimola, P., Ragnelli, A. M., Pacioni, G., & Miranda,
621 M. (2011). Tyrosinase expression during black truffle development: From free living
622 mycelium to ripe fruit body. *Phytochemistry*, *72*(18), 2317–2324.
623 https://doi.org/10.1016/j.phytochem.2011.08.025

624 Zarivi, O., Cesare, P., Ragnelli, A. M., Aimola, P., Leonardi, M., Bonfigli, A., Colafarina, S.,
625 Poma, A. M., Miranda, M., & Pacioni, G. (2015). Validation of reference genes for
626 quantitative real-time PCR in Périgord black truffle (*Tuber melanosporum*)
627 developmental stages. *Phytochemistry*, *116*(1), 78–86.
628 https://doi.org/10.1016/j.phytochem.2015.02.024

629 Zeppa, S., Gioacchini, A. M., Guidi, C., Guescini, M., Pierleoni, R., Zambonelli, A., &
630 Stocchi, V. (2004). Determination of specific volatile organic compounds synthesised
631 during *Tuber borchii* fruit body development by solid-phase microextraction and gas
632 chromatography/mass spectrometry. *Rapid Communications in Mass Spectrometry*,
633 *18*(2), 199–205. https://doi.org/10.1002/RCM.1313

634

635

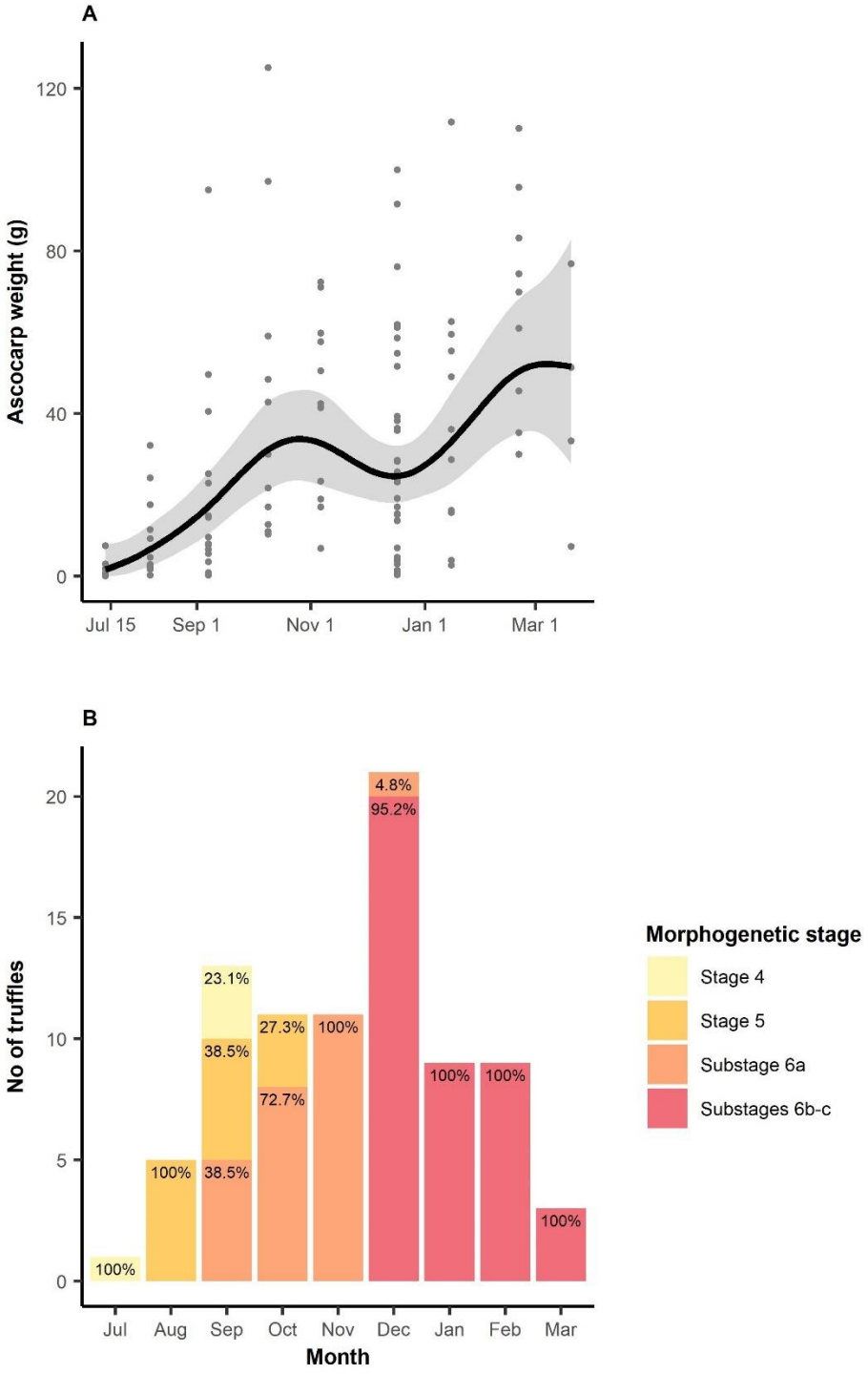

Figure 1. (a) Predicted evolution (mean and 95% confidence band, n = 83) of the fresh weight of *Tuber melanosporum* ascocarps from July to March. Points represent partial residuals. (b) Number (and percentage) of *T. melanosporum* ascocarps in each morphogenetic stage for each sampling (n = 83). See Table 1 for the description of the morphogenetic stages.

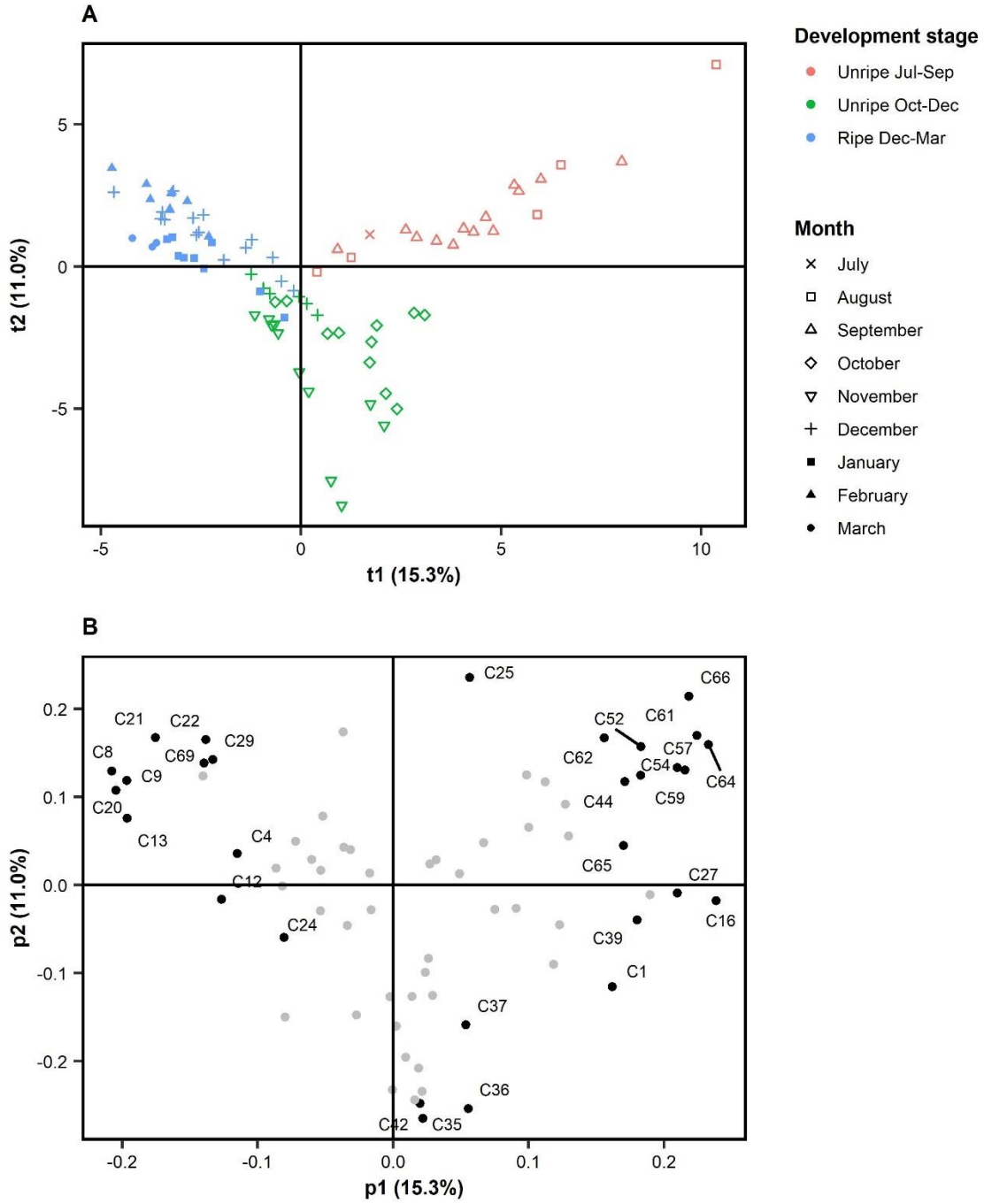

641

642 **Figure 2**. Results of the PLS-DA analyzing the VOC profile in black truffle according to the
643 development stage (unripe ascocarps in July-September, unripe ascocarps in October-
644 December, and ripe ascocarps in December-March): (a) scores plot of the samples, (b) loading
645 plot of the VOCs, with those having VIP_{pred} higher than one in black (n = 83). The VOCs are
646 named according to the IDs in Table 2.

647

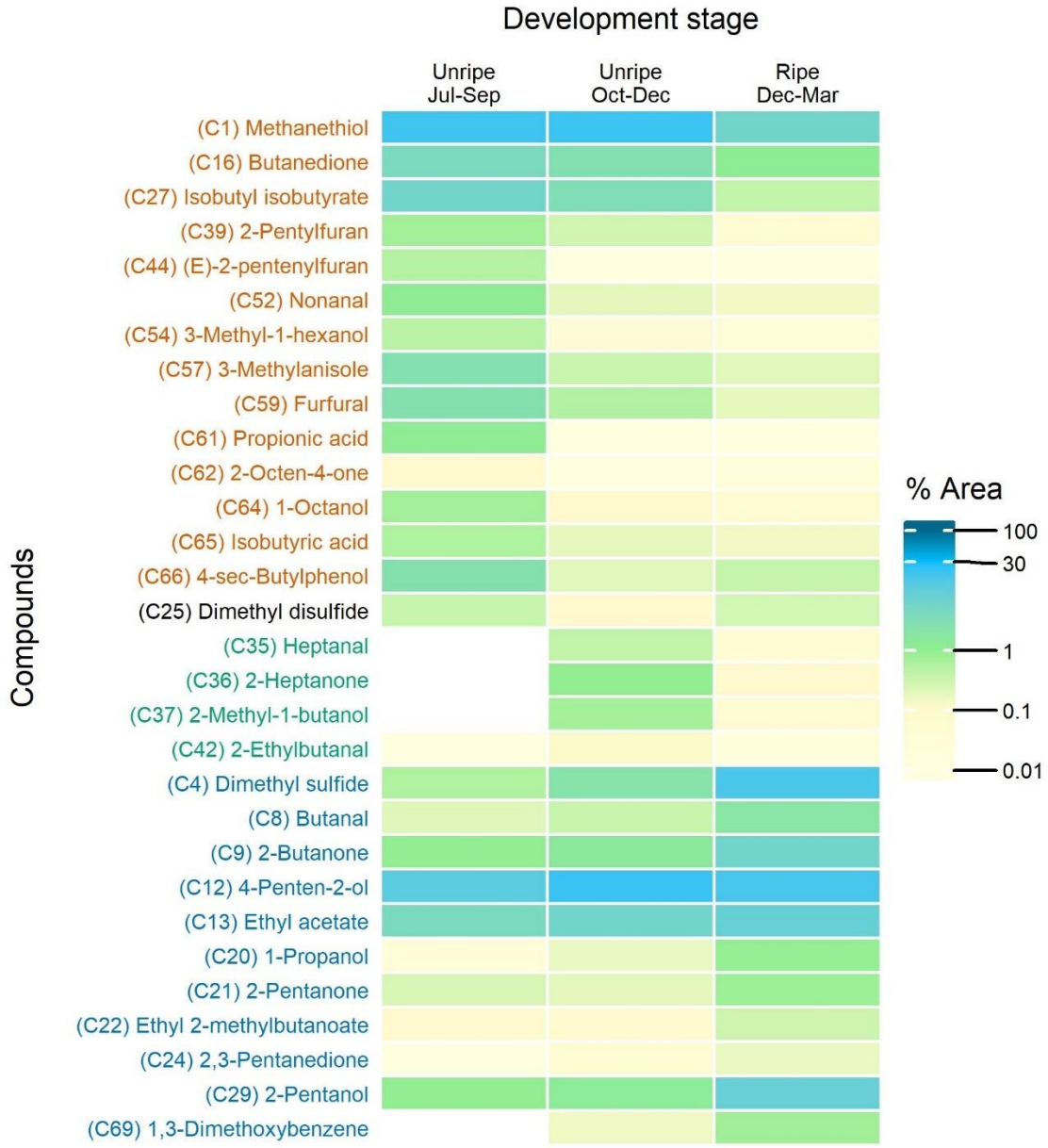

Figure 3. Heatmap of the relative area (%) for VOCs with VIP_{pred} higher than one, in the three development stages (n = 19, 28 and 35 for each stage). Compounds in red and blue are positively and negatively associated with the first PLS-DA component. Compounds in black and green are positively and negatively associated with the second PLS-DA component, correspondingly. Percent area in logarithmic scale.

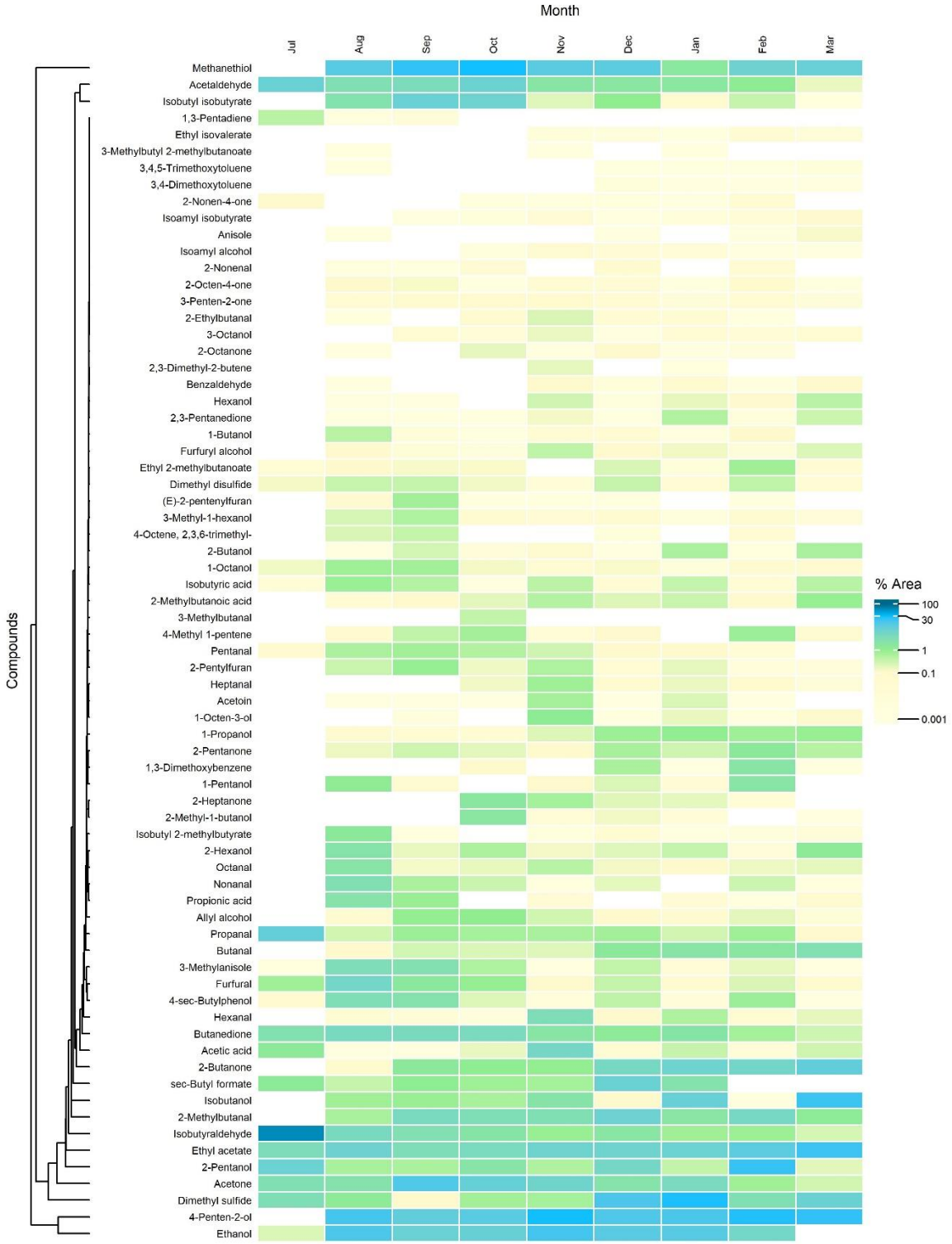

Figure 4. Heatmap of the relative area (%) for all volatile organic compounds, in the nine monthly samplings (n = 1, 5, 13, 11, 11, 21, 9, 9 and 3 for each month correspondingly). Compounds are clustered according to a divisive hierarchical clustering. Percentage area in logarithmic scale.

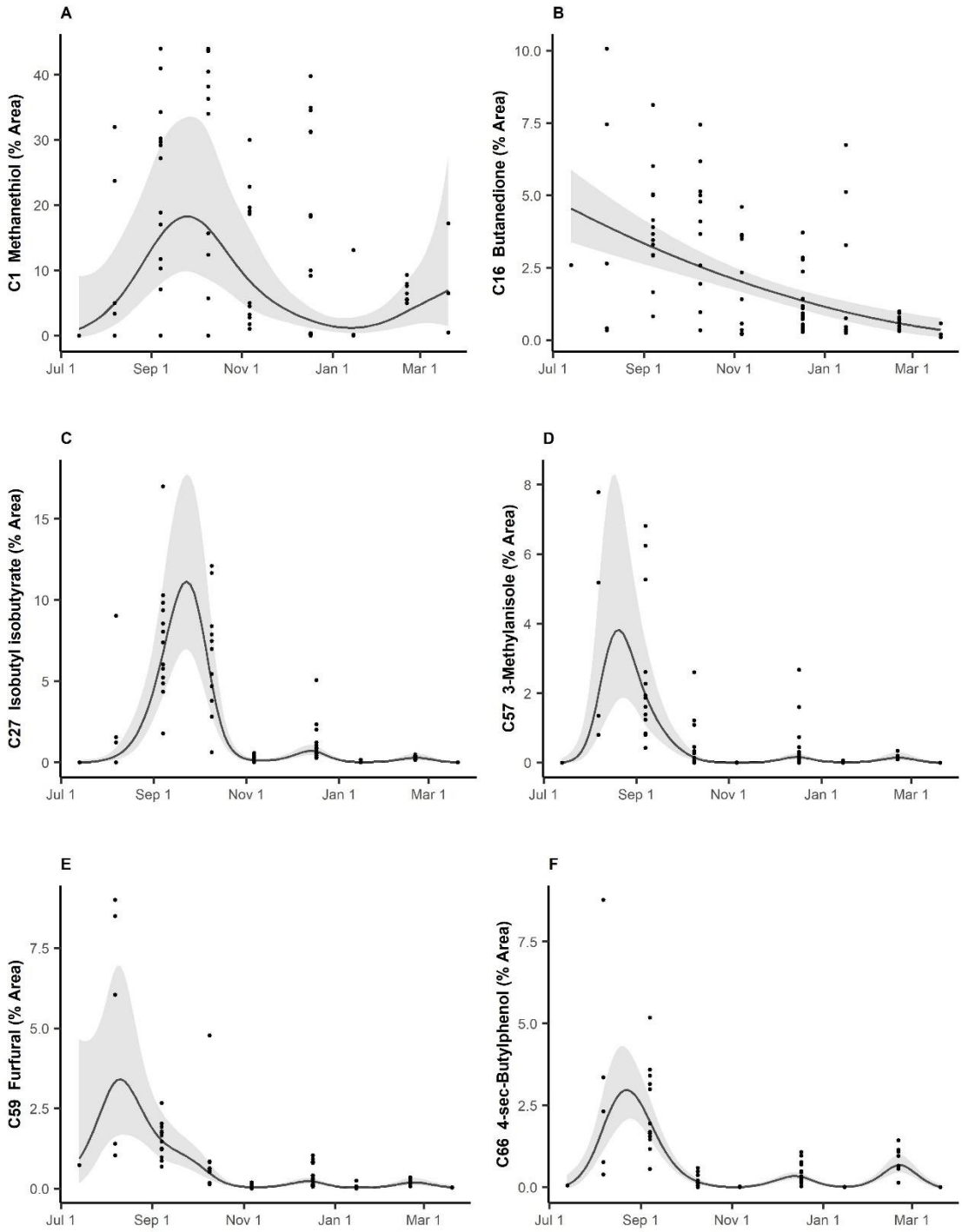

661

662 **Figure 5**. Predicted evolution (mean and 95% confidence band, n = 83) of relative area (%)
663 throughout the development of truffle, for the most frequent VOCs positively associated to
664 unripe truffles according to VIP_{pred} scores: (a) methanethiol, (b) butanedione, (c) isobutyl
665 isobutyrate, (d) 3-methylanisole, (e) furfural and (f) 4-sec-butylphenol. Points represent
666 partial residuals. Notice that the y-axis scale of each panel is different.

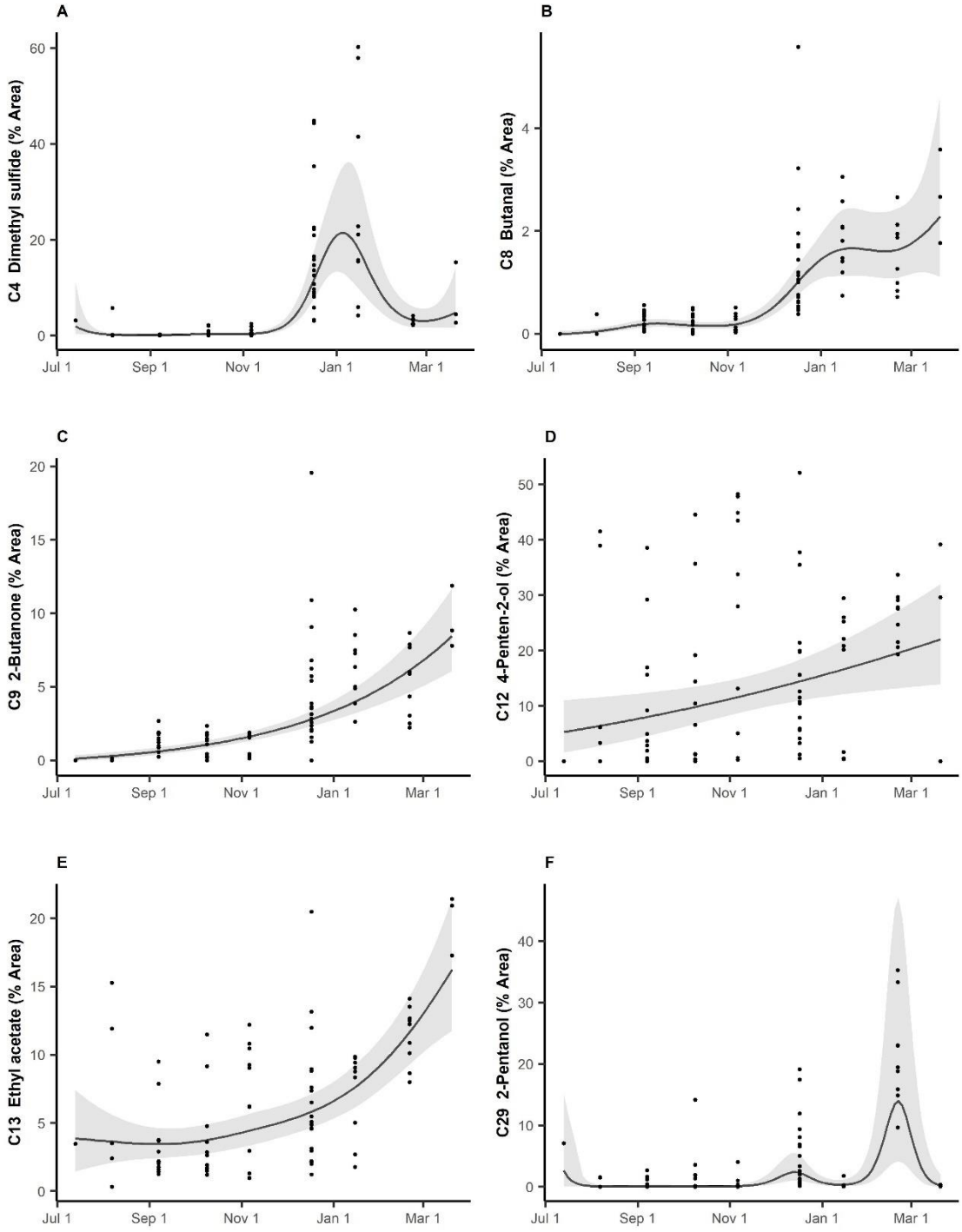

Figure 6. Predicted evolution (mean and 95% confidence band, n = 83) of relative area (%) throughout the development of truffle, for the most frequent VOCs positively associated to ripe truffles according to VIP_{pred} scores: (a) dimethyl sulfide, (b) butanal, (c) 2-butanone, (d) 4-penten-2-ol, (e) ethyl acetate and (f) 2-pentanol. Points represent partial residuals. Notice that the y-axis scale of each panel is different.

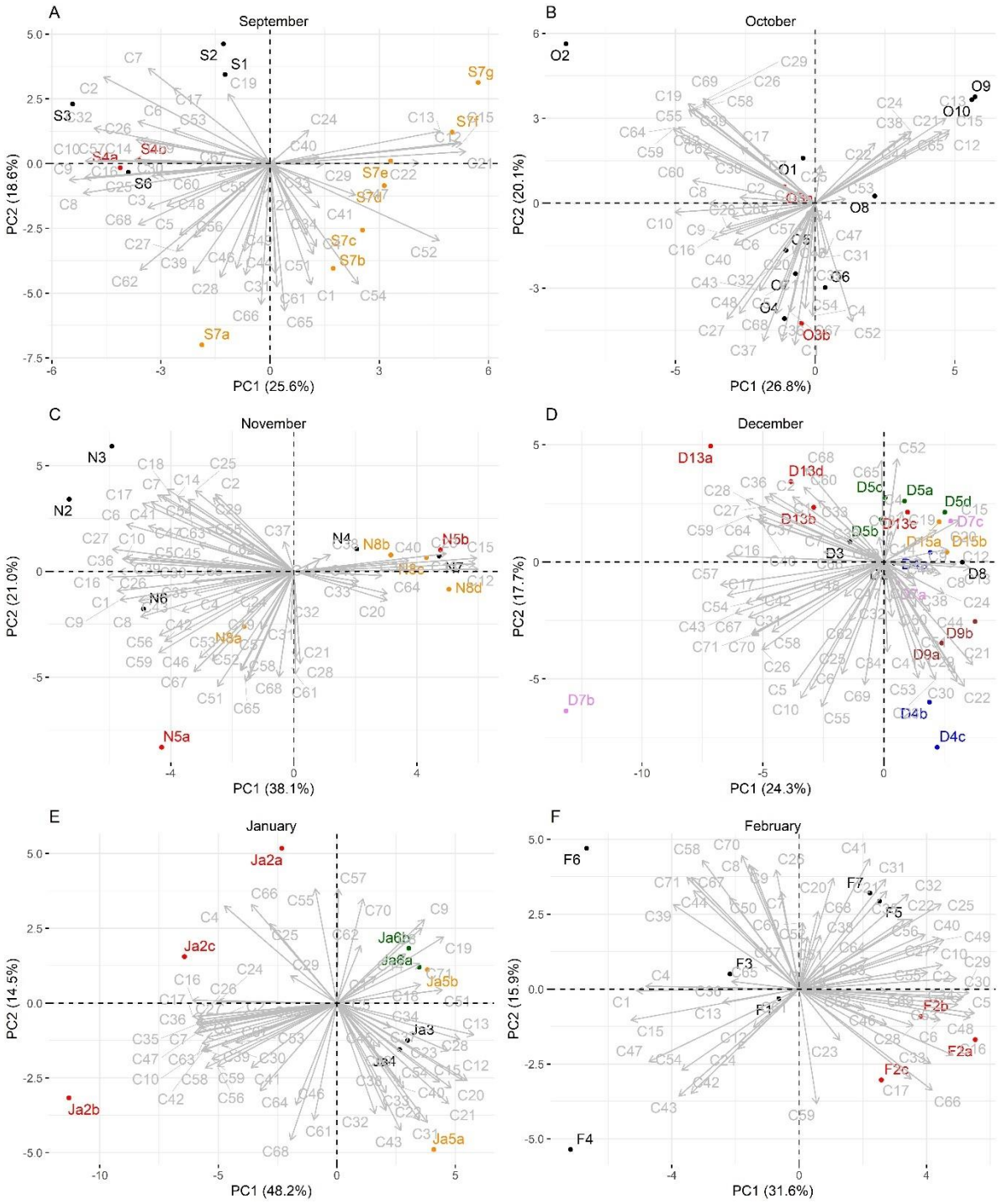

673

674 **Figure 7**. PCA biplots for the VOC profile of truffle ascocarps of September (a), October (b),

675 November (c), December (d), January (e) and February (f). Digs with only one ascocarp

676 (single ascocarps) are named with only a number, digs with multiple ascocarps (ascocarp

677 clusters) are named with a number and a letter. Each cluster is labeled with a different color.

678 In December, single ascocarps and clusters 2 to 9 were marked by trained dogs, whereas

679 clusters 13 and 15 were not. The VOCs are named according to the IDs in Table 2.

680

681

682

683 **Table 1**. Morphogenetic stages according to Zarivi et al. (2015) and Le Tacon (2017)

Stage	Description
Stage 1 (hyphal)	The ascocarps consist of a cluster of poorly differentiated hyphae.
Stage 2 (peridial)	Outer hyphae of the ascocarp form a finely warty initial peridium. Below them, hyphae form an initial gleba, largely folded-convoluted.
Stage 3 (veined)	Gleba whitish-marbled and veins increasingly complex and compact. No asci discernible.
Stage 4 (ascal)	Fertile veins containing asci. No ascospores discernible.
Stage 5 (sporal)	Ascospores hyaline (visible cell content), with smooth walls or beginning to develop spines.
Stage 6 (pigmented)	
Substage 6a	Spores with ornamentation completely formed, most spores hyaline or slightly pigmented. Fertile veins yellowish, faint aroma.
Substages 6b-c	Spores mainly dark brown. Fertile veins brown to dark brown, intense aroma. Substage 6c involves the beginning of over-ripening processes, such as brown pigmentation extending to sterile veins, the occurrence of which is related to the frequency of harvesting.

684

685

686 **Table 2**. HS-GC-MS characteristics of volatile organic compounds found in the samplings.
687 CAS No: CAS registry number. RT: retention time. RI_{exp}: experimental retention index. RI_{lit}:
688 reference retention according to NIST database. NA: not available. Odor attributes were
689 selected following Acree & Arn (2004) and Tejedor-Calvo et al. (2021).

Id.	Compound	Odor attribute	CAS No	RT (min)	RI_{exp}	RI_{lit}	Mass (m/z)
Acids							
C58	Acetic acid	Sour	64-19-7	16.88	1455	1452	43
C61	Propionic acid	Pungent, rancid, soy	79-09-4	18.13	1538	1540	74
C65	Isobutyric acid	Rancid, butter, cheese	79-31-2	18.59	1571	1570	43
C68	2-Methylbutanoic acid	Cheese, sweat	116-53-0	19.96	1674	1674	74
Esters							
C13	Ethyl acetate	Pineapple	141-78-6	6.60	907	900	43
C14	sec-Butyl formate	-	589-40-2	6.80	919	NA	45
C22	Ethyl 2-methylbutanoate	Apple	7452-79-1	9.01	1042	1052	102
C23	Ethyl isovalerate	Fruit	108-64-5	9.34	1058	1053	88
C27	Isobutyl isobutyrate	-	97-85-8	9.80	1081	1092	71
C33	Isobutyl 2-methylbutyrate	-	2445-67-2	11.42	1459	1179	85
C34	Isoamyl isobutyrate	-	2050-01-3	11.70	1172	1183	70
C45	3-Methylbutyl 2-methylbutanoate	-	27625-35-0	14.21	1297	1276	70
Aldehydes							
C2	Acetaldehyde	Pungent, ether	75-07-0	4.01	722	714	44
C5	Propanal	Solvent, pungent	123-38-6	5.30	800	799	58
C6	Isobutyraldehyde	Pungent, malt, green	78-84-2	5.45	813	818	72
C8	Butanal	Pungent, green	123-72-8	5.92	853	877	72
C10	2-Methylbutanal	Cocoa, almond	96-17-3	6.20	876	903	57
C11	3-Methylbutanal	Malt	590-86-3	6.30	885	906	44
C17	Pentanal	Almond, malt, pungent	110-62-3	7.82	979	982	44
C26	Hexanal	Grass, tallow, fat	66-25-1	9.58	1070	1072	44
C35	Heptanal	Fat, citrus, rancid	111-71-7	11.85	1179	1183	70
C42	2-Ethylbutanal	-	97-96-1	13.42	1257	NA	43
C47	Octanal	Fat, soap, lemon, green	124-13-0	14.62	1320	1297	43
C52	Nonanal	Fat, citrus, green	124-19-6	15.73	1384	1392	57
C60	2-Nonenal	Paper	2463-53-8	18.00	1533	1533	43
Ketones							
C7	Acetone	-	67-64-1	5.60	825	820	43
C9	2-Butanone	Ether	78-93-3	6.00	864	866	43
C16	Butanedione	Butter	431-03-8	7.79	978	975	43
C21	2-Pentanone	Ether, fruit	107-87-9	8.70	1026	1025	43
C24	2,3-Pentanedione	Cream, butter	600-14-6	9.35	1059	1052	43
C31	3-Penten-2-one	-	625-33-2	10.82	1130	1138	69
C36	2-Heptanone	Soap	110-43-0	11.92	1182	1180	43
C43	2-Octanone	Soap, gasoline	111-13-7	13.80	1279	1278	43
C46	Acetoin	Butter, cream	513-86-0	14.40	1310	1287	45
C55	2-Nonen-4-one	-	32064-72-5	16.66	1441	1466	84
C62	2-Octen-4-one	-	4643-27-0	18.21	1544	NA	69
Alcohols							
C12	4-Penten-2-ol	-	625-31-0	6.50	901	NA	45
C15	Ethanol	Sweet	64-17-5	7.30	949	935	45
C19	2-Butanol	Wine	78-92-2	8.36	1009	1022	59
C20	1-Propanol	Alcohol, pungent	71-23-8	8.60	1021	1025	59
C28	Isobutanol	Wine, solvent, bitter	78-83-1	10.02	1092	1095	43
C29	2-Pentanol	Green	6032-29-7	10.30	1106	1117	45
C30	Allyl alcohol	-	107-18-6	10.61	1120	1124	57
C32	1-Butanol	Fruit	71-36-3	10.85	1132	1148	56
C37	2-Methyl-1-butanol	Wine, onion	137-32-6	12.31	1201	1208	57
C38	Isoamyl alcohol	Whiskey, malt, burnt	123-51-3	12.40	1206	1212	55
C40	2-Hexanol	-	626-93-7	12.70	1221	1245	45
C41	1-Pentanol	Balsamic	71-41-0	13.35	1254	1255	42
C51	Hexanol	Resin, flower, green	111-27-3	15.30	1359	1359	56
C53	3-Octanol	Moss, nut, mushroom	589-98-0	15.91	1394	1397	59
C54	3-Methyl-1-hexanol	-	13231-81-7	16.25	1415	1413	55
C56	1-Octen-3-ol	Mushroom	3391-86-4	16.78	1448	1453	57
C64	1-Octanol	Chemical, metal, burnt	111-87-5	18.43	1560	1560	56
Hydrocarbons							
C3	1,3-Pentadiene	-	504-60-9	4.41	746	743	67
C18	2,3-Dimethyl-2-butene	-	563-79-1	8.14	998	NA	41
C48	4-Methyl 1-pentene	-	691-37-2	14,88	1335	NA	43
C49	2,3,6-Trimethyl-4-octene	-	63830-65-9	15.03	1344	NA	69
Aromatic compounds							

C50	Anisole	-	100-66-3	15.11	1348	1340	108
C57	3-Methylanisole	-	100-84-5	16.85	1453	1441	122
C63	Benzaldehyde	Almond, burnt sugar	100-52-7	18.25	1547	1547	106
C66	4-sec-Butylphenol	-	99-71-8	19.27	1621	NA	121
C69	1,3-Dimethoxybenzene	-	151-10-0	21.15	1771	1762	138
C70	3,4-Dimethoxytoluene	-	494-99-5	21.72	1818	1806	152
C71	3,4,5-Trimethoxytoluene	-	6443-69-2	25.12	>2000	2041	182
Hetercyclic compounds							
C39	2-Pentylfuran	Green bean, butter	3777-69-3	12.68	1220	1228	81
C44	(E)-2-pentenylfuran	-	70424-14-5	14.12	1293	1282	107
C59	Furfural	Bread, almond, sweet	98-01-1	17.23	1477	1470	96
C67	Furfuryl alcohol	Burnt	98-00-0	19.89	1668	1668	81
Sulfur-containing compounds							
C1	Methanethiol	Sulfur, gasoline, garlic	74-93-1	3.90	715	699	47
C4	Dimethyl sulfide	Cabbage, sulfur, gasoline, truffle	75-18-3	4.94	778	760	62
C25	Dimethyl disulfide	Onion, cabbage, putrid, truffle	624-92-0	9.52	1067	1069	94

690